

DESIGN AND EXPERIMENT ON SEED-GUIDING TUBE OF T-GROOVE FURROWING DEVICE BASED ON BRACHISTOCHRONE

基于最速降线的 T 型槽开沟装置导种管设计与试验

Chenxi HE¹); Xiunan JIN¹); Liquan LU¹); Mengliang MA¹); Xinxin WANG¹); Junchang ZHANG^{*1});

¹College of Mechanical and Electronic Engineering, Northwest A&F University, Yang ling 712100/ China;

Tel: +86 13759898701; E-mail: zhangjc@nwfau.edu.cn

DOI: <https://doi.org/10.35633/inmateh-67-05>

Keywords: Seed-guiding tube; Brachistochrone; Seeding uniformity; Discrete element

ABSTRACT

The disorder flow of seeds caused by the collision in the seed-guiding tube is one of the important reasons for the reduction of seeding uniformity. For this problem, a seed-guiding tube with brachistochrone considering the influence of friction was presented in this paper. By analyzing kinetics and rotating the equation coordinate system, brachistochrone under the condition of friction was obtained and applied to the design of the structural parameters of the grain conductor of T-groove furrowing device, and a discrete element model of the grain conductor and wheat was established, thus single-factor simulation analysis and quadratic regression orthogonal rotation combination simulation tests were conducted to explore the optimal combination of parameters. The test results showed that the seed-guiding tube had a brachistochrone radius of 14.708 mm, a linear length of 500 mm and a working speed of 4 km/h, and the seed spacing offset dispersion degree and the seed lateral offset dispersion degree were 12.26 and 8.53 respectively, which had a high seeding uniformity. The results of the bench validation test showed that the coefficients of variation of the two test evaluation indexes between the bench test results and the virtual simulation results were 10.20% and 8.62% respectively, therefore the simulation results could be used for the optimization of the seed guide tube.

摘要

种子在导种管内因碰撞引起的种子无序流动是导致排种均匀性降低的重要原因之一，针对该问题，本文设计了一种考虑摩擦影响的最速降线导种管。通过动力学分析与旋转方程坐标系等方法得到了考虑摩擦条件下的最速降线，并将其应用于 T 型槽开沟装置导种管的结构参数设计中，建立了导种管与小麦离散元模型，进行单因素仿真分析与二次回归正交旋转组合仿真试验探究最优参数组合。试验结果表明，导种管最速降线旋轮半径为 14.708mm、直线段长度为 500mm、工作速度为 4km/h 时，粒距偏移离散度和种粒横向偏移离散度分别为 12.26 与 8.53，具有较高的排种均匀性。台架验证性试验结果表明，台架试验结果与虚拟仿真结果的两项试验评价指标变异系数分别为 10.20%、8.62%，仿真结果能够用于导种管的优化。

INTRODUCTION

The structural parameters of the seed-guiding tube have a great influence on the collision of seedpods in the pipe during seed-guiding process, and the collision between seeds and between seeds and grain conductor is the main reason to destroy the uniform and orderly movement state of seedpods and lead to the low uniformity of seeding (Kocher *et al.*, 2011; Sharma and Pannu, 2014). Many scholars have conducted a lot of research on grain conductor for improving seeding uniformity. Based on theoretical analysis of seedpod motion state and mathematical modeling of grain conductor shape, Liu Xiaomin and Deng Jiangyu proposed that a reasonable shape of seed-guiding tube should be composed of three segments: brachistochrone - inclined straight line – brachistochrone (Liu X M and Deng, 1987). Zhong Yunlong *et al.* applied the theory of brachistochrone and proposed a seed-guiding tube consisting of two curves of parabolic line and brachistochrone, which could reduce the movement time of seedpods in the pipe and make seedpods have a better landing speed and angle (Zhong *et al.*, 2011). Zhao Shuhong *et al.* designed a maize seed-guiding device by combining the brachistochrone with a V-groove, which effectively improved seed row uniformity by constraining the seedpod movement trajectory (Zhao *et al.*, 2018).

¹ Chenxi, He, M.D. Stud. Eng.; Xiunan, Jin, M.D. Eng.; Liquan, Lu, M.D. Stud. Eng.;

Mengliang, Ma, M.D. Stud. Eng.; Xinxin, Wang, M.D. Stud. Eng.; Junchang Zhang, Assoc. Prof. M.D. Eng.

The above studies showed that the application of brachistochrone to the design of seed-guiding devices can reduce the collision between seeds and between seeds and the tube wall by reducing the gliding time of seedpods in the grain conductor, which is conducive to ensuring a uniform and orderly seed flow and effectively improving the seed row uniformity. However, the above-mentioned studies have not considered the effect of friction on brachistochrone when applying brachistochrone to the design of the seed-guiding components. Neglecting the effect of friction will lead to a significant decrease in the effect of brachistochrone (i.e., the minimum time used for the mass to slide along brachistochrone between two points) (Shi *et al.*, 2020), thus, it is necessary to further study it.

The T-groove seed and fertilizer separating furrowing device for wheat is a new type of furrow opening device, which is based on the wide and narrow row sowing mode, and can realize double row sowing and fertilizer side deep application in one opening. The device has two long L-shaped seed-guiding tubes. In this paper, brachistochrone considering the friction condition is applied to the design of grain conductor of this device, and the optimal structure and working parameter combination of the seed-guiding tube are derived through simulation analysis and experimental research, in order to provide reference for the design of new seed-guiding components.

MATERIALS AND METHODS

T-groove furrowing device structure and working principle

T-groove seed and fertilizer separating furrowing device for wheat mainly consists of vertical knife, horizontal knife, shovel handle, fertilizer-discharging tube, seed-guiding tube and seed-guiding tube clamping device, as shown in Figure 1. The operation process is shown in Fig. 2. The vertical knife opens the fertilizer trench, the shovel handle is hollow and also serves as the fertilizer-discharging pipe, the fertilizer falls into the fertilizer trench along the pipe, realizing the side deep application of fertilizer, the horizontal knives on both sides of the vertical knife open the seed trench on both sides above the fertilizer trench, the seeds fall into the seed trench along the grain conductor hidden under the horizontal knife, and the trench is opened once to realize double row sowing and seed fertilizer application.

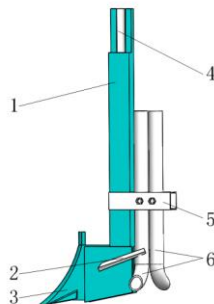


Fig. 1 - The wheat T-groove seed and fertilizer separating furrowing device

1 - shovel handle; 2 - horizontal knife; 3 - vertical knife;
4 - fertilizer-discharging tube; 5 - seed-guiding tube clamping device;
6 - seed-guiding tube

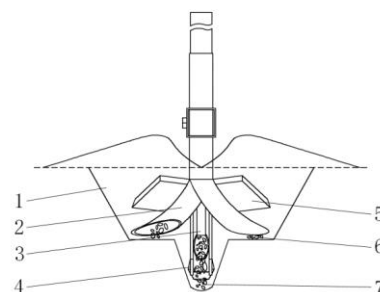


Fig. 2 - Working process of the T-groove furrowing device

1 - fertilizer trench; 2 - seed-guiding tube;
3 - fertilizer-discharging tube; 4 - shovel handle;
5 - horizontal knife; 6 - wheat seeds ; 7 - fertilizer

Design of brachistochrone segment of seed-guiding tube

The brachistochrone problem is a particle that is only affected by gravity and has zero initial velocity sliding from a point A along a smooth curve to any point B not in its vertical direction, and the time it takes to slide is the shortest, its analytical equation is (Xing and Yang, 2019):

$$\begin{cases} x = r(\theta - \sin\theta) \\ y = r(1 - \cos\theta) \end{cases} \quad (1)$$

(x,y) – particle coordinates, [mm];

θ – the angle of rotation of the particle when it rolls, [°]

In engineering, the effect of friction on brachistochrone needs to be considered, so as to avoid ignoring the effect of friction that causes the shortest time to glide to be greatly reduced (*Shi et al., 2020*). Assuming that the friction coefficient between the seedpod and the wall of the seed-guiding tube is μ , the effect of centrifugal force can be ignored due to the small curvature of the designed brachistochrone (*Liu X M and Deng, 1987*), then the change of the kinetic energy of the seedpod is:

$$d\left(\frac{mv^2}{2}\right) = mgdy - \mu mg\cos\varphi ds = mgd(y - \mu_x) \quad (2)$$

m – quality of seedpod, [kg];

g – gravitational acceleration, [m/s²];

μ – coefficient of dynamic friction between seedpod and wall of seed-guiding tube;

φ – friction angle between seedpod and wall of seed-guiding tube, [°];

s – seedpod movement distance, [mm]

After the seed leaves the seed meter, it slides down the curve of the seed-guiding tube, and its movement speed is:

$$v = \sqrt{2g(y - \mu_x)} + v_0 \quad (3)$$

v_0 – velocity of seed when it reaches the curved section of the seed-guiding tube, [m/s]

The time taken for the seedpod to slide from point A to point B is:

$$T = \int_0^{x_B} F dx = \int_0^{x_B} \frac{\sqrt{1+(y')^2}}{\sqrt{2g(y-\mu_x)+v_0}} dx \quad (4)$$

x_B – horizontal coordinate of point B, [mm]

The problem of the steepest descent line considering the influence of frictional resistance is to find the extremum curve of time T . Eliminating the friction coefficient in the velocity function can be achieved by rotating the equation coordinate system (*You, 2005*).

As shown in Figure 3, rotate the A - xy coordinate system by the friction angle φ in the clockwise direction to obtain the coordinate system A - XY , where $\varphi = \arctan \mu$, then there is:

$$y - \mu_x = \frac{Y}{\cos\varphi} \quad (5)$$

Therefore, equation (4) can be rewritten as:

$$T = \int_0^B \frac{ds}{v} = \int_0^{X_B} \frac{\sqrt{1+Y'^2}}{\sqrt{(2g/\cos\varphi)Y+v_0}} dX \quad (6)$$

(X, Y) – coordinates of seedpod after rotating the coordinate system, [mm];

X_B – horizontal coordinate of point B after rotating the coordinate system, [mm]

On the brachistochrone (Fig.3), l_a , the speed of the seed in the AD section is lower than the speed when it is in free fall. Therefore, the brachistochrone l_a into the A - xy coordinate system $x < 0$ area cannot make the glide time T get the minimum value, that is, non-optimal path. In the A - xy coordinate system, the optimal path exists between the y -axis and the straight-line $y = \mu x$, so the scaling and translation transformation is performed on the formula (1).

$$\begin{cases} X = R(\theta - \sin\theta) + b \\ Y = R(1 - \cos\theta) \end{cases} \quad (7)$$

R – parameter after transformation, [mm];

b – equation lateral translation amount, [mm]

After the transformation, the movement path is that the seed particle from point A along the y-axis for free fall motion to point C, and then slide along the brachistochrone l_b to point B. At this time, the movement time is:

$$T = \sqrt{\frac{2y_C}{g}} + \int_{x_C}^{x_B} F dx = \sqrt{\frac{2y_C}{g}} + \int_{x_C}^{x_B} \frac{\sqrt{1+Y'^2}}{\sqrt{2g(y-\mu x)+v_0}} dx \tag{8}$$

(x_C, y_C) – coordinate of point C, [mm]

When the position of the boundary point C changes, there is:

$$\delta T = \frac{1}{\sqrt{2gy_C}} \left(1 - \frac{y'}{\sqrt{1+y'^2}} \right) \delta y_C \tag{9}$$

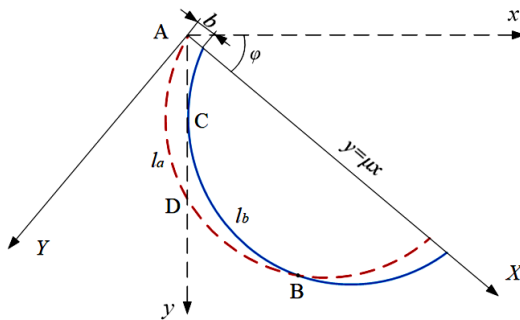


Fig. 3 - Brachistochrone after rotating the coordinate system

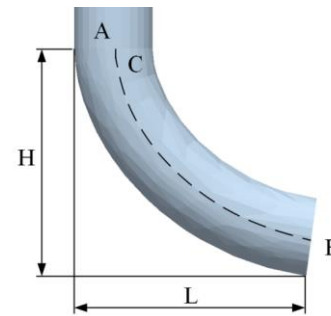


Fig. 4 - Section of the Brachistochrone of seed-guiding tube

When the boundary point C is the extreme point, there should be $\delta T = 0$, $y' = \infty$, that is, the brachistochrone tangent to the y-axis. Therefore, when the brachistochrone l_b is tangent to the y-axis, the line segment is the brachistochrone between the two points A and B under the action of friction. The tangent point, i.e., the boundary point C, should satisfy:

$$\begin{cases} \frac{dY}{dX} \Big|_C = \frac{1-\cos\theta_C}{\sin\theta_C} = \mu \\ X_C = R(\theta_C - \sin\theta_C) + b \\ Y_C = R(1 - \cos\theta_C) + b \\ X_C = \mu Y_C \end{cases} \tag{10}$$

(X_C, Y_C) – coordinates of point C after rotating the coordinate system, [mm];

θ_C – parameter angle of the pendulum at the tangent point C, [°]

From formula (10), there is:

$$\mu = \tan\left(\frac{\theta_C}{2}\right) \tag{11}$$

Since the brachistochrone from A to B is composed of a straight line along the y-axis direction and a brachistochrone l_b tangent to it when friction is considered, the angle between the bottom of the brachistochrone and the horizontal direction is φ , therefore, the corresponding brachistochrone parameter angle at the tangent point C is:

$$\theta_C = 2 \arctan \mu = 2\varphi \tag{12}$$

Then, the lateral translation amount of the brachistochrone equation is obtained as:

$$b = R[(\mu^2 + 1) \sin\theta_C - \theta_C] = 2R(\mu - \arctan\mu) \tag{13}$$

It can be seen from equations (7) and (13) that the brachistochrone parameters R and b between points A and B only depend on the relative positions of points A and B and the friction factor between the seedpod and the inner wall of the seed-guiding tube. Among them, the relative position between points A and B is the spatial position between the beginning of the brachistochrone segment of the grain conductor and the end of the grain conductor, as shown in Figure 4. The brachistochrone is composed of a straight line AC and a brachistochrone CB when friction is considered, and the upper part of the grain conductor is composed of a straight line, so the transition between the straight section of the grain conductor and the brachistochrone section will not cause the increase of the seed collision.

According to the structural characteristics of the T-groove furrowing device, in order to facilitate the seed-guiding tube to be hidden under the horizontal knife of the furrowing device and meet the requirements of wide and narrow row seeding row spacing, the longitudinal spacing H between points A and B should be less than 50 mm, and the lateral spacing L should be 50 mm. Based on this, the range of values of the radius R of the brachistochrone and the angle θ of the rotating wheel with it can be determined.

Discrete Element Simulation Analysis

In order to explore the influence of the structural parameters and operating parameters of seed-guiding tube on the seeding uniformity, and to optimize the structural parameters of tube, a discrete element simulation study was carried out on the seeding process of the tube.

● Simulation model establishment of seed-guiding tube and wheat seeds, etc.

SolidWorks 2018 was used to create a 3D model of the seed-guiding tube and it was imported into EDEM 2018, as shown in Figure 5, and the material of the pipe was set to ABS plastic. Using the Northwest A&F University's No.585 wheat cultivar as the prototype of discrete element modeling, the geometric size of seedpods was measured and statistically analyzed, and the results are shown in Table 1.

Statistical analysis results of the three axis dimensions of the seedpod

Table 1

Item	Maximum value / (mm)	Minimum value (mm)	Average value (mm)	Standard deviation	Coefficient of variation / (%)	P-value (S-W)
Long axis	7.22	5.82	6.43	0.27	4.20	0.851
Center axis	3.80	2.87	3.39	0.20	5.90	0.102
Short axis	3.64	2.63	3.11	0.22	7.07	0.727

Based on the measurement and analysis results, the ellipsoidal model of wheat seeds was constructed with seven-sphere filling.

The initial velocity of seeds was set as 0.3 m/s and the direction was along the gravity direction (Li, 2009). The discrete element simulation model is shown in Figure 6.

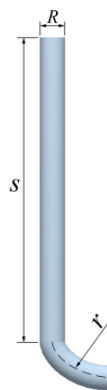


Fig. 5 - 3D model of the seed-guiding tube
 R – diameter; s - straight line length; r - radius of brachistochrone



Fig. 6 - DEM simulation model
1 - particle factory; 2 – seed-guiding tube; 3 – soil

To simplify the simulation model, the seed meter is replaced by setting the simulation parameters of the particle factory in this paper, and particle factory is set at the entrance of grain conductor. Based on the characteristics of Northwest A&F University's No.585 wheat cultivar and different working speeds and seed metering device rotational speeds in the actual sowing operation, the calculated rate of seedpods produced by particle factory is shown in Table 2 (Jin, 1996).

Table 2

Working speed / (km·h ⁻¹)	Number of seeds / (particle·s ⁻¹)	Seeding rate / (s· particle ⁻¹)
4	49	0.02027
5	62	0.01620
6	74	0.01347
7	86	0.11571

● Simulation parameter setting

The Hertz-Mindlin (no slip) contact model was used for the simulation analysis of wheat seeds and seed-guiding tube (Zhai, 2018). In order to be as close as possible to the actual soil environment of the seed furrow and the environment of seeding belt with seeding oil on bench test stand, the simulation soil model uses cohesive soil, and the material parameters and contact parameters required for the simulation were obtained from relevant literature, as shown in Table 3 and Table 4 (Hang, 2017; Huang et al., 2016; Liu F Y et al., 2016; Xiang et al., 2019; Zhang et al., 2021).

Table 3

Materials	Poisson's ratio	Density / (kg·m ⁻³)	Shear modulus / MPa
Wheat	0.29	1350	501
ABS plastic	0.394	1060	896
Soil	0.38	2680	1.2

Table 4

Contact form	Restitution coefficient	Static friction coefficient	Rolling friction coefficient
Wheat–wheat	0.46	0.58	0.08
Wheat–ABS plastic	0.02	1.26	1.24
Wheat–soil	0.14	0.33	0.2

● Determination of simulation evaluation indexes

In order to quantify the seeding uniformity of the seed-guiding tube designed based on the principle of brachistochrone, the dispersion degree of seed spacing offset and the dispersion degree of seed lateral offset were used as evaluation indicators for analysis (Guo et al., 2020).

The dispersion degree of seed spacing offset: refers to the offset degree between the distance x between projections of seeds on the axis (i.e. actual grain distance) and the theoretical grain spacing. It is an important index to evaluate the longitudinal distribution of seed grains in the seed bed.

The calculation formula is as in equation (14).

$$\sigma = \sqrt{\frac{1}{N} \sum_{i=1}^N (x_i - \mu)^2} \tag{14}$$

σ – seed spacing offset dispersion degree;

N – total number of grain spacing;

x_i – actual grain distance, [mm];

μ – theoretical grain distance, [mm].

The dispersion degree of seed lateral offset: refers to the degree of grain offset from the axis, is an important index to evaluate the lateral distribution of grains in the seed bed. The vertical distance y of the grain from the origin axis is its lateral offset, and the calculation formula is as in equation (15).

$$\bar{d} = \frac{\sum_{i=1}^n |y_i - \bar{y}|}{n} \tag{15}$$

\bar{d} – average absolute deviation;

y_i – lateral offset of seeds, [mm];

\bar{y} – offset average, [mm];

n – total number of offsets

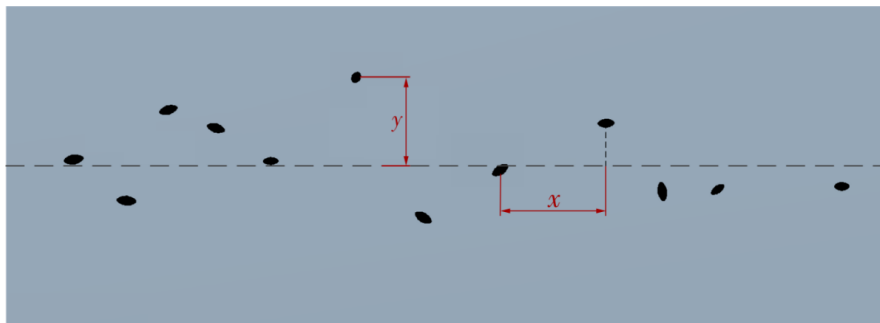


Fig. 7 - Diagram of test indicators

● **Single-factor simulation analysis**

In order to narrow the level range of the test factors in the orthogonal simulation test, the single-factor test was carried out on the test factors by the control variable method to determine the initial preferred range of test factor parameters.

The straight section length of seed-guiding tube s , the radius of brachistochrone r and working speed v are the important parameters affecting the seeding uniformity, and the above three parameters were selected as the test factors to analyze the influence law of each factor on the seeding uniformity. According to the characteristics of wheat seeds as small grain seeds, the diameter of the grain conductor was selected as 20 mm. The factors and levels of the single-factor test were selected as shown in Table 5.

Table 5

Single factor test factor and level table

Level	Straight section length of seed-guiding tube/(mm)	Radius of brachistochrone/(mm)	Working speed /(km/h)
1	350	13.9	4
2	400	15.9	5
3	450	17.9	6
4	500	19.9	7
5	550	21.9	-

● Secondary orthogonal simulation test

In order to further analyze the influence of the structure and working parameters of the grain conductor on the seeding uniformity, based on the single-factor simulation analysis, a 3-factor, 3-level quadratic orthogonal rotational combination test was used to analyze the interaction law between the straight section length of seed-guiding tube s , the radius of brachistochrone r and the working speed v on the test evaluation indexes, using the seed spacing offset dispersion degree and the seed lateral offset dispersion degree as the test evaluation indexes. The orthogonal test factor levels are shown in Table 6.

Table 6

Orthogonal test factor level table

Level	Straight section length of seed-guiding tube / (mm)	Radius of brachistochrone / (mm)	Working speed / (km/h)
-1	400	13.9	4
0	450	15.9	5
1	500	17.9	6

● Bench test

In order to verify the optimization results of the simulation test, a bench validation test was conducted. The seeds used in the test were Northwest A&F University's No.585 wheat seeds, and the 3D printing method was used to process the trial seed-guiding tube, whose structural parameters were: the length of linear section of grain conductor was 500 mm, the diameter was 20 mm, and the radius of brachistochrone was 14.708 mm. The test was conducted in the agricultural machinery laboratory of the Mechanical and Electronic Engineering College of Northwest A&F University, and the equipment used was the Heilongjiang Agricultural Machinery Scientific Research Institute developed JPS-12 seed rower performance testing test bench. The forward speed of the belt of seed bed was set to 4 km/h to simulate the actual working speed of the seed-guiding tube. The bench test setup is shown in Figure 8, and the above test parameters were used to repeat the test five times.

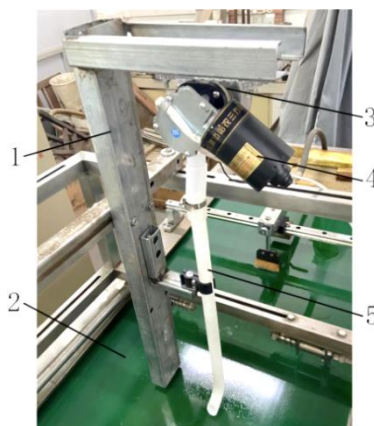


Fig. 8 - Bench test equipment

1 - seed metering device bracket; 2 - seeding belt; 3 - seed metering device; 4 - motor; 5 - seed-guiding tube

RESULTS

Single-factor simulation test results and analysis

(1) Influence of the straight section length of seed-guiding tube on the test evaluation index

It can be seen from Fig. 9a that the dispersion degree of seed spacing offset varied greatly under different lengths of linear section of the seed-guiding tube.

With the increase of the linear length of the pipe, the overall trend of dispersion degree of seed spacing offset is rising and then falling, and is at the lowest level at 500 mm, about 11.20 mm. The dispersion degree of seed lateral offset shows a trend of first decrease and then ascend with the increase of the straight section length of tube, and is at the lowest level at 400 mm, about 6.40 mm.

Under the condition that it cooperates with the T-groove furrowing device, it is necessary to further study the effect of the interaction between the linear length of pipe of 400 mm~500 mm and other factors on the uniformity of seeding.

(2) Influence of the radius of brachistochrone on the test evaluation index.

As can be seen from Figure 9b, with the increase of the radius of brachistochrone, both the dispersion degree of seed spacing offset and the dispersion degree of seed lateral offset showed an overall descending trend followed by a rising trend, and both evaluation indexes reach the lowest level at the radius of brachistochrone of about 15.9 mm, which is about 12.24 mm and 6.37 mm respectively. The smaller the radius of brachistochrone is, the better the seed-guiding tube is hidden under the horizontal knife of the furrowing device. Under the condition of favorable grain conductor hiding, the effect of the interaction between the radius of brachistochrone of 13.9 mm~17.9 mm and other factors on the seeding uniformity needs to be further studied.

(3) Influence of working speed on test evaluation index

It can be seen from Fig. 9c that the dispersion degree of seed spacing offset increases with the rise of working speed; the dispersion degree of seed lateral offset goes up first and then declines with the increase of working speed. Both indexes are at the lowest level when the working speed was 4 km/h, about 12.33 mm and 6.04 mm respectively. Considering the working efficiency and seeding quality, it is necessary to further study the effect of the interaction between the working speed of 4 km/h~6 km/h and other factors on the seeding uniformity.

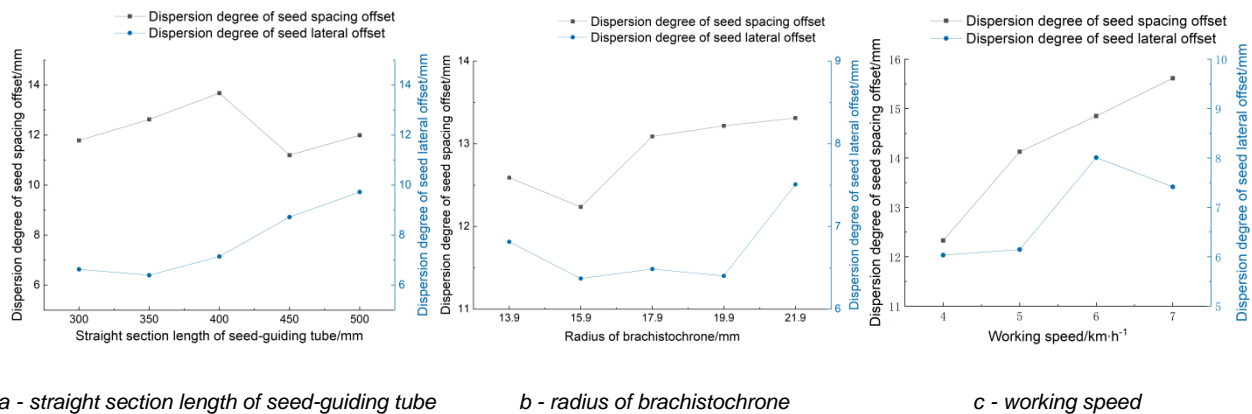


Fig. 9 - The influence of test factors on test evaluation indexes

Orthogonal test results and analysis

● Results of the orthogonal test and its analysis of variance

The orthogonal test design scheme and results are shown in Table 7. Analysis of variance was performed on the experimental data using Design-Expert 12 software, and the results are shown in Table 8. From the analysis results, it can be seen that the influence of test factors on the dispersion degree of seed spacing offset in descending order is working speed *C*, radius of brachistochrone *B*, and straight section length of seed-guiding tube *A*. The influence of radius of brachistochrone B^2 on the dispersion degree of seed spacing offset is the most significant in the secondary term. The influence of test factors on the dispersion degree of seed lateral offset in descending order is working speed *C*, straight section length of seed-guiding tube *A*, and radius of brachistochrone *B*. The effect of straight section length of pipe and radius of brachistochrone *AB* on the dispersion degree of seed lateral offset is highly significant in the interaction term, and the effect of radius of brachistochrone B^2 on the dispersion degree of seed lateral offset is most significant in the secondary term.

● Influence of interaction factors on experimental evaluation indexes

Response surface graph was drawn by Design-Expert software to analyze the influence of the pairwise interaction between *A*, *B*, and *C* factors on the response values Y_1 and Y_2 .

(1) Analysis of the effect of interaction factors on the dispersion degree of seed spacing offset

As shown in Fig. 10a, when the working speed is 5 km/h, as the radius of brachistochrone increases, the dispersion degree of seed spacing offset goes down with the increase of the straight section length of tube, which is similar to the research results of Liu Jianying et al (Liu J Y et al., 2016).

The main reason is that when the linear section length of tube is about 500 mm, with the augment of the seed movement time, the movement state of the seeds in the latter part of the grain conductor tends to be stable, and the minimum velocity in the movement process occurs near the exit of the pipe, so the seeds bounce and displace less after contacting the ground, which leads to a smaller dispersion degree of seed spacing offset. In the process of increasing the straight section length of tube, the dispersion degree of seed spacing offset tends to decline and then rise with the increase of the radius of brachistochrone.

As shown in Fig. 10b, when the radius of brachistochrone is 15.9 mm, the dispersion degree of seed spacing offset decreases with the increase of the linear length of grain conductor when the working speed rises, and the overall decrease is not significant. In the process of increasing the linear length of tube, the dispersion degree of seed spacing offset goes up with the increase of working speed.

As shown in Fig. 10c, when the straight section length of tube is 450 mm, with the rise of working speed, the dispersion degree of seed spacing offset is falling and then ascending with the increase of the radius of brachistochrone. The reason for this is that when the radius of brachistochrone is in the middle level, the angle between the tangent line at the end of the curve and the horizontal direction is a suitable landing angle for the seedpods, and the seeds moving along the curve are influenced by the curvature of the curve, which changes the movement direction of the seeds, so that the seedpods have a good landing angle when they leave pipe, and the displacement after landing is smaller, which leads to a smaller dispersion degree of seed spacing offset. When the radius of brachistochrone increases, the dispersion degree of seed spacing offset goes up with the rise of working speed, and the trend is approximately linear.

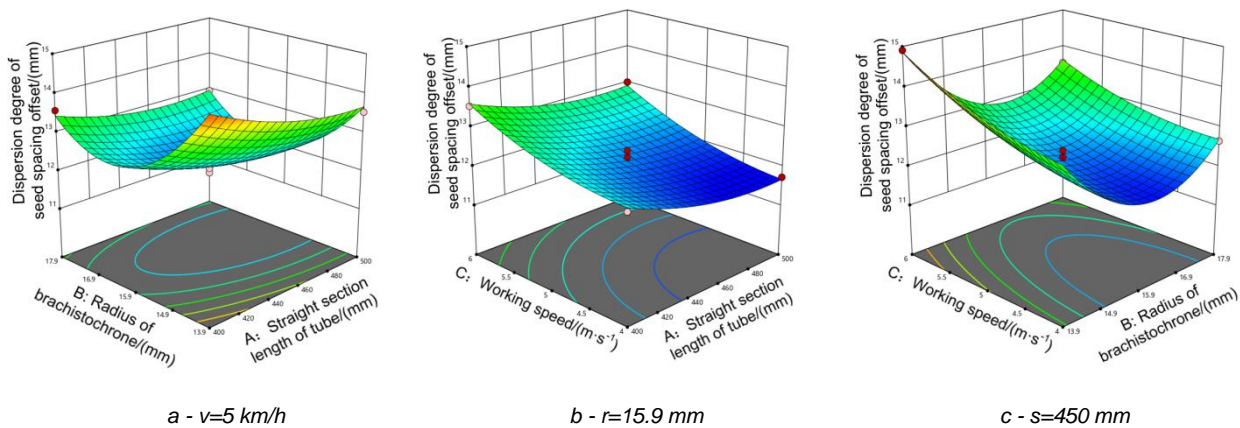


Fig. 10 - The influence of interaction factors on dispersion degree of seed spacing offset

Table 7

Experimental design plan and results

Test Serial number	Test factors			Test evaluation index	
	Straight section length of tube	Radius of brachistochrone	Working speed	Dispersion degree of seed spacing offset	Dispersion degree of seed lateral offset
	<i>I</i> A	<i>I</i> B	<i>I</i> C	<i>Y</i> ₁	<i>Y</i> ₂
1	500	15.9	6	12.96	10.77
2	450	15.9	5	13.54	8.09
3	450	15.9	5	13.54	11.52
4	450	15.9	5	12.07	11.53
5	450	15.9	5	11.73	10.56
6	400	15.9	6	13.57	7.97
7	450	15.9	5	12.24	11.83
8	450	13.9	6	13.56	9.67

9	400	13.9	5	12.42	12.01
10	500	17.9	5	14.71	10.90
11	500	15.9	4	14.91	11.30
12	450	17.9	6	11.96	12.12
13	400	15.9	4	12.66	8.37
14	450	17.9	4	13.54	8.09
15	450	13.9	4	13.02	12.19
16	500	13.9	5	12.07	11.50
17	400	17.9	5	12.40	9.43

Table 8

Analysis of variance

Source	Dispersion degree of seed spacing offset				Dispersion degree of seed lateral offset			
	Sum of Square	Degree of freedom	F-value	P-value	Sum of Square	Degree of freedom	F-value	P-value
Model	13.66	9	50.82	< 0.0001**	36.97	9	30.17	< 0.0001**
A	1.11	1	37.25	0.0005**	0.4028	1	2.96	0.1291
B	1.94	1	64.88	< 0.0001**	0.3193	1	2.35	0.1695
C	2.76	1	92.45	< 0.0001**	8.48	1	62.25	< 0.0001**
AB	0.0768	1	2.57	0.1529	7.9	1	58.01	0.0001**
AC	0.0059	1	0.1989	0.6691	0.0514	1	0.3777	0.5583
BC	0.0559	1	1.87	0.2136	0.9136	1	6.71	0.0359*
A ²	0.3123	1	10.45	0.0144*	0.6701	1	4.92	0.062
B ²	6.77	1	226.48	< 0.0001**	16.28	1	119.59	< 0.0001**
C ²	0.2518	1	8.43	0.0229**	0.951	1	6.98	0.0333*
Residual	0.2091	7			0.9532	7		
Lack of Fit	0.0804	3	0.8329	0.5415	0.6401	3	2.73	0.1786
Pure Error	0.1287	4			0.3131	4		
Cor Total	13.87	16			37.92	16		

*** indicates that the item is highly significant ($P < 0.01$); * indicates that the item is significant ($P < 0.05$)

(2) Analysis of the effect of interaction factors on the dispersion degree of seed lateral offset

When the working speed is 5 km/h, the interaction effect between the radius of brachistochrone and the straight section length of grain conductor is shown in Fig. 11a. The dispersion degree of seed lateral offset descends with the rise of the linear length of pipe when the radius of brachistochrone increases. In the process of rising the straight section length of tube, the dispersion degree of seed lateral offset tended to increase and then decline with the increase of the radius of brachistochrone, and the decrease is significant at the larger radius of brachistochrone.

Figure 11b shows the interaction effect between the working speed and the straight section length of tube when the radius of brachistochrone is 15.9 mm. With the rise of working speed, the dispersion degree of seed lateral offset ascends slowly with the increase of the straight section length of pipe, and the overall fluctuation range is not significant. In the process of increasing the linear length of grain conductor, the dispersion degree of seed lateral offset showed an upward trend with the rise of working speed.

When the straight section length of seed-guiding tube is 450 mm, the interaction effect of working speed and the radius of brachistochrone is shown in Fig. 11c. In the process of increasing the working speed, the dispersion degree of seed lateral offset tended to go up and then fall with the rise of the radius of brachistochrone. With the increase of the radius of brachistochrone, the dispersion degree of seed lateral offset ascended with the rise of working speed, and the ascent showed a slowing trend. The reason for the ascent of the dispersion degree of seed lateral offset due to the increase of working speed is that the increase of working speed makes the seedpods have a larger horizontal parting speed, which rises the displacement of seeds after leaving pipe and causes a larger dispersion degree of seed lateral offset.

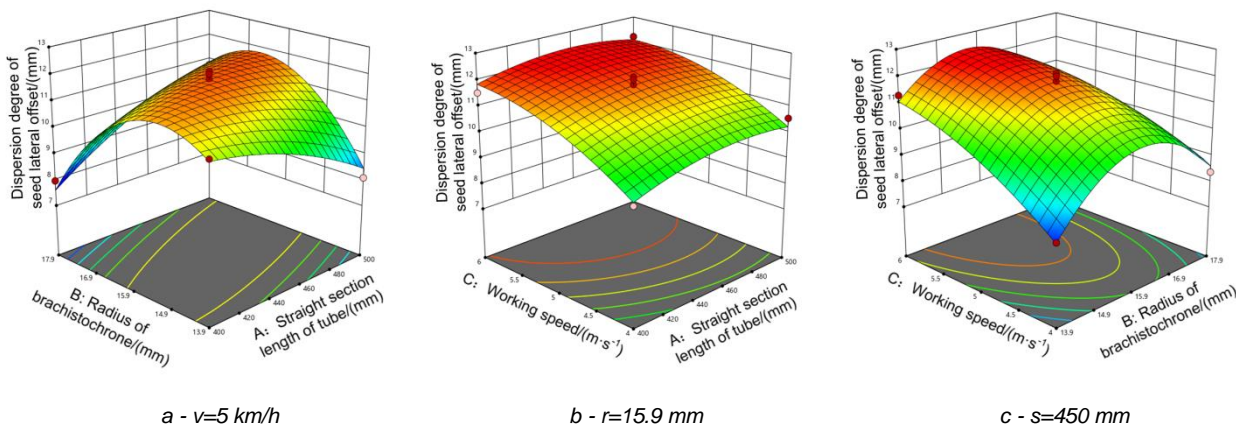


Fig. 11 - The influence of interaction factors on dispersion degree of seed lateral offset

● **Parameter optimization**

The above research results show that the straight section length of seed-guiding tube, the radius of brachistochrone, and the working speed will affect the uniformity of seeding. In order to obtain the optimal parameter combination of the seed-guiding tube structure and working parameters of the T-groove furrowing device, the multi-objective optimization method is adopted. According to the actual working conditions and model analysis results, the optimization constraint is set as formula (16). Combined with the importance of the influence of dispersion degree of seed spacing offset and dispersion degree of seed lateral offset on seeding quality, the importance of dispersion degree of seed spacing offset is set to the highest level, followed by dispersion degree of seed lateral offset.

$$\begin{cases} \min Y_1(A, B, C) \\ \min Y_2(A, B, C) \\ \text{s.t.} \begin{cases} 400 \leq A \leq 500 \\ 13.9 \leq B \leq 17.9 \\ 4 \leq C \leq 6 \end{cases} \end{cases} \quad (42)$$

Based on the Optimization module of the Design-Expert software, the parameters are optimized and analyzed. It can be seen that when the straight section length of seed-guiding tube is 500 mm, the radius of brachistochrone is 14.708 mm, and the working speed is 4 km/h, the dispersion degree of seed spacing offset and dispersion degree of seed lateral offset are 12.26 mm and 8.53 mm respectively.

Analysis of bench test results

Through 5 repeated tests, the results of the bench verification test are that dispersion degree of seed spacing offset is 10.61 mm, and the dispersion degree of seed lateral offset is 7.55 mm. The coefficients of variation of the two test evaluation indexes between the bench test and the virtual simulation results are 10.20% and 8.62%, and the bench test results are basically consistent with the virtual simulation results, which means that the simulation results can be used for the optimization of the seed-guiding tube.

CONCLUSIONS

(1) In order to solve the problem of seed collision in seed-guiding tube causing disorderly flow of seeds and thus reducing seeding uniformity, brachistochrone was applied to the design of grain conductor. By analyzing kinetics and rotating the equation coordinate system, brachistochrone was obtained under the condition of friction, and the structural parameters of the seed-guiding tube of the T-groove furrowing device was designed by using it as the shape of the curved section of the grain conductor, and the sliding time of seedpods was reduced in the seed guide tube to reduce the collision of the seeds in the tube and improve seeding uniformity.

(2) Single-factor simulation analysis and quadratic regression orthogonal rotational combination simulation tests were conducted with the straight section length of the seed-guiding tube, the radius of brachistochrone and the working speed as the test factors, and the dispersion degree of seed spacing offset and the dispersion degree of seed lateral offset as the test indexes. The test results showed that the grain conductor had a radius of brachistochrone of 14.708 mm, a linear length of 500 mm and an operating speed of 4 km/h, and the seed spacing offset dispersion degree and the seed lateral offset dispersion degree were 12.26 mm and 8.53 mm respectively, which had a high uniformity of seeding.

(3) The bench validation test was conducted, and the test results showed that the bench test results were basically consistent with the virtual simulation results, and the coefficients of variation of the two test evaluation indexes were 10.20% and 8.62% respectively, and the simulation results could be used for the optimization of the seed-guiding tube.

ACKNOWLEDGEMENT

The work in this paper was supported by the Key Research and Development Program of Shaanxi Province (No. 2020NY-119).

REFERENCES

- [1] Guo Hui, Wang Gang, Zhao Jiale, Jia Honglei, Yuan Hongfang, Huang Dongyan, (2020), Seed longitudinal distribution uniformity index and seed spatial distribution uniformity evaluation method (种子纵向分布均匀性指标及空间分布均匀性评价方法), *Journal of Jilin University (Engineering and Technology Edition)*, Jilin / Jilin, vol. 50, No. 3, ISSN 1671-5497, pp. 1120-1130.
- [2] Hang Chengguang, (2017), *Soil Disturbance Behavior of Subsoiling Based on Discrete Element Method (基于离散元方法的深松土壤扰动行为研究)*, Master Thesis, Northwest A&F Univ., Yangling / Shannxi.
- [3] Huang Yuxiang, Hang Chengguang, Yuan Mengchan, Wang Botao, Zhu Ruixiang, (2016), Discrete Element Simulation and Experiment on Disturbance Behavior of Subsoiling (深松土壤扰动行为的离散元仿真与试验), *Transactions of the Chinese Society of Agricultural Machinery*, Chaoyang / Beijing, vol. 47, No. 7, ISSN 1000-1298, pp. 80-88.
- [4] Jin Shangbao, (1996), *Chinese wheat science (中国小麦学)*, China Agricultural Press, Beijing, 613 p., ISBN 7-109-03782-7/S-2384.
- [5] Kocher, M.F., Coleman, J.M., Smith, J.A., Kachman, S.D., (2011), Corn seed spacing uniformity as affected by seed tube condition, *Applied Engineering in Agriculture*, Michigan / St. Joseph, vol. 27, No. 1, ISSN 0883-8542, pp. 177-183.
- [6] Li Zhengquan, (2009), *Study on Digital Design Method of Wheat Metering Device based on DEM (基于离散元法的小麦排种器的数字化设计方法研究)*, Master Thesis, Jilin University, Changchun / Jinlin.
- [7] Liu Xiaomin, Deng Jiangyu, (1987), Theoretical Analysis of the Reasonable Shape of the Seed Tube of the High Speed Precision Planter (高速精密播种机导种管合理形状的理论分析), *Journal of Agricultural Mechanization Research*, Harbin / Heilongjiang, No. 1, ISSN 1003-188X, pp. 35-39.
- [8] Liu Jianying, Zhang Pengju, Liu Fei, (2016), The Discrete Element Simulation Guide Tube Height Effects on Seeding Performance (离散元模拟导种管高度对排种性能的影响), *Journal of Agricultural Mechanization Research*, Harbin / Heilongjiang, vol. 38, No. 1, ISSN 1003-188X, pp. 12-16.
- [9] Liu Fanyi, Zhang Jian, Li Bo, Chen Jun, (2016), Calibration of parameters of wheat required in discrete element method simulation based on repose angle of particle heap (基于堆积试验的小麦离散元参数分析及标定), *Transactions of the Chinese Society of Agricultural Engineering*, Chaoyang / Beijing, vol. 32, No. 12, ISSN 1002-6819, pp. 247-253.

- [10] Shi Naiyu, Chen Haitao, Wei Zhipeng, Chai Yuduo, Hou Shouyin, Wang Xing, (2020), Design and Test of Forced-return Device Based on Principle of Brachistochrone (基于最速降线原理的免耕播种机强制回土装置研究), *Transactions of the Chinese Society of Agricultural Machinery*, Chaoyang / Beijing, vol. 51, No. 2, ISSN 1000-1298, pp. 37-44.
- [11] Sharma, S., Pannu, C.J.S., (2014) Development and Evaluation of Seed Metering System for Water Soaked Cotton Seeds, *Ama-Agricultural Mechanization in Asia Africa and Latin America*, Chiyoda-Ku / Tokyo, vol. 45, No. 1, ISSN 0084-5841, pp. 41-47.
- [12] Xiang Wei, Wu Mingliang, Lv Jiangnan, Quan Wei, Ma Lan, Liu Jianjie, (2019), Calibration of simulation physical parameters of clay loam based on soil accumulation test (基于堆积试验的黏壤土仿真物理参数标定), *Transactions of the Chinese Society of Agricultural Engineering*, Chaoyang / Beijing, vol. 35, No. 12, ISSN 1002-6819, pp. 116-123.
- [13] Xing Jiasheng, Yang Yichuan, (2019), Proof of Sufficient Conditions for Brachistochrone Problem Solution (最速降线问题解的充分条件的证明), *Journal of Jishou University (Natural Science Edition)*, Jishou / Hunan, vol. 40, No. 2, ISSN 1007-2985, pp. 1-4.
- [14] You Qingming, (2005), Study on the solution of brachistochrone and the effect of friction (最速降线求解和摩擦力影响的研究), *Journal of Henan Polytechnic University (Natural Science Edition)*, Jiaozuo / Henan, vol. 24, No. 1, ISSN 1007-7332, pp. 83-88.
- [15] Zhai Mengmeng, (2018), *Optimum Design and Test of Wheat Wide Precision Seeding Device Based on EDEM (基于 EDEM 的小麦宽幅精量播种装置优化设计与试验)*, Master Thesis, Shandong Agricultural University, Taian / Shandong.
- [16] Zhao Shuhong, Chen Junzhi, Wang Jiayi, Chen Jiaqi, Yang Chao, Yang Yunqian, (2018), Design and Experiment on V-groove Dialing Round Type Guiding-seed Device (精量播种机 V 型凹槽拨轮式导种部件设计与试验), *Transactions of the Chinese Society of Agricultural Machinery*, Chaoyang / Beijing, vol. 49, No. 6, ISSN 1000-1298, pp. 146-158.
- [17] Zhang Shun, Li Yong, Wang Haoyu, Liao Juan, Li Zhaodong, Zhu Dequan, (2021), Design and experiment on the seed spout of inside-filling pneumatic type precision hole-seeding meter device for rice (水稻内充气力式精量穴播排种器导种管的设计与试验), *Journal of Hunan Agricultural University (Natural Sciences)*, Changsha / Hunan, vol.47, No. 1, ISSN 1007-1032, pp. 71-80.
- [18] Zhong Yunlong, Zhang Yongliang, Yan Junchao, Hu Jianping, Wu Yaodong, (2011), Design and Research of the Curve of Seed Tub in Co-operation Machine of Rotary Tiller Fertilization Sowing (旋耕灭茬施肥播种联合作业机导种管设计), *Journal of Agricultural Mechanization Research*, Harbin / Heilongjiang, vol. 33, No. 12, ISSN 1003-188X, pp. 98-99+105.